

macQsimal	Title	Deliverable Number D8.2
Project Number 820393	Quantification of bandwidth and sensitivity of Rb sensor for different sample volumes	Version 1

H2020-FETFLAG-2018-2021

macQsimal

Miniature Atomic vapor-Cell Quantum devices for SensIng and Metrology AppLications

Deliverable D8.2

Quantification of bandwidth and sensitivity of Rb sensor for different sample volumes

WP8 - Rydberg gas sensors

Authors: Robert Löw, Harald Kübler, Fabian Munkes, Patrick Kaspar, Tilman Pfau (STUTT)

Lead participant: STUTT

Delivery date: 09.04.2021

Dissemination level: Public

Type: R (Document, Report)



This work has received funding from the European Union's Horizon 2020 research and innovation programme under grant agreement No. 820393.

macQsimal	Title	Deliverable Number D8.2
Project Number 820393	Quantification of bandwidth and sensitivity of Rb sensor for different sample volumes	Version 1

Revision History

Author Name, Partner short name	Description	Date
Robert Löw (STUTT) Harald Kübler (STUTT) Fabian Munkes (STUTT) Patrick Kaspar (STUTT) Tilman Pfau (STUTT)	Draft deliverable (Draft 1)	15.02.2021
Johannes Ripperger (accelCH)	Checks on formalities and layout	19.02.2021
Jacques Haesler (CSEM)	Revision 1	23.02.2021
Janine Riedrich-Möller (BOSCH) Tino Fuchs (BOSCH)	Revision 2	12.03.2021
Robert Löw (STUTT)	Final version	01.04.2021

Abbreviations

N2	Nitrogen
NO	Nitric oxide
Rb	Rubidium
WP	Work Package
ITO	Indium tin oxide
MFC	Mass flow controller

Partner short names

accelCH	accelopment Schweiz AG, CH
CSEM	CSEM SA – Centre Suisse d'Électronique et de Microtechnique, CH
STUTT	Universität Stuttgart, DE
BOSCH	Robert Bosch GmbH, DE

macQsimal	Title	Deliverable Number
Project Number 820393	Quantification of bandwidth and sensitivity of Rb sensor for different sample volumes	D8.2
		Version 1

Contents

1	INTRODUCTION	5
2	HIGH RESOLUTION RYDBERG SPECTROSCOPY	5
2.1	General scheme Rb.....	5
2.2	Results of Rb sensors.....	5
2.3	General scheme NO (For details please refer to D8.1)	8
2.4	Vapour cell with current detection	9
2.5	Data acquisition.....	10
2.6	Outlook.....	10

macQsimal	Title	Deliverable Number
Project Number 820393	Quantification of bandwidth and sensitivity of Rb sensor for different sample volumes	D8.2
		Version 1

Executive Summary

This deliverable reports on the influence of the cell size and electrode size on the sensitivity and the bandwidth of device for the Rb sensor. Due to the COVID-19 crisis we decided to extract the performance of the Rb gas sensor based on our data acquired so far. Additional experiments have not been performed due to limitations in laboratory accessibility. To make an advance here we started earlier to investigate this very same topic for the NO sensor. This deliverable will be partially merged with the deliverable D8.3 “Quantification of bandwidth and sensitivity of NO sensor for different sample volumes”.

Need for the Deliverable

The objective of this deliverable was to benchmark the already further developed Rb sensor. From these specifications we planned to translate our findings to the NO sensor. But during our investigations we found that the gas flow of Rb cannot be compared to that of NO and we can only draw first conclusions for the performance of our first NO sensor setups.

Objectives of the Deliverable

The objective has been to collect knowledge of gas flow dynamics and the performance of the amplifying units for Rb sensors. As this is only partially doable, we will report here mostly on the electronics, and the gas flow for the NO sensor.

Outcomes

We performed a series of experiments for the Rb gas sensor. The main outcome here is that we cannot talk about a classical gas flow as the rubidium tends to stick on the walls and performs rather a random walk, in spite of the classical molecular gas flow set by the background gas (here N₂). Therefore, we cannot conclude anything from this on the performance of the NO gas sensor. But we have tested first electrode setups and trans-impedance amplifiers. In our first version we chose trans-impedance amplifiers (for Rb and NO) with a rather large input resistance (>MegaOhm), which makes the detection scheme not so sensitive to the capacity or the inductance of the electrodes. The input resistance dominates the system.

Next steps

We will have to find in an experiment the absolute limits of our setups. For now, it is not clear where an optimum operation can be performed. This depends also on the requested specifications we want, whether the gas flow, the gas volume, the bandwidth or the sensitivity is in the focus. Each application will lead to a different design. For the rest of this project we aim on cm³ sized volumes with a bandwidth in the high kHz regime.

macQsimal	Title	Deliverable Number D8.2
Project Number 820393	Quantification of bandwidth and sensitivity of Rb sensor for different sample volumes	Version 1

1 Introduction

This deliverable reports on the progress made on the setup of a trace-gas sensor for rubidium and nitric oxide based on Rydberg excitations. Such a Rydberg gas sensor will benefit current small sized and integrable systems that are now limited to a few gases of interest. In the medical context of breath analysis, one molecule of interest is nitric oxide (NO), which is an indicator for several severe conditions. The main aspect here is the influence of the cell size and other dimensions of the setup (tubing, electronics, field plates) on the performance of the sensor.

2 High resolution Rydberg spectroscopy

2.1 General scheme Rb

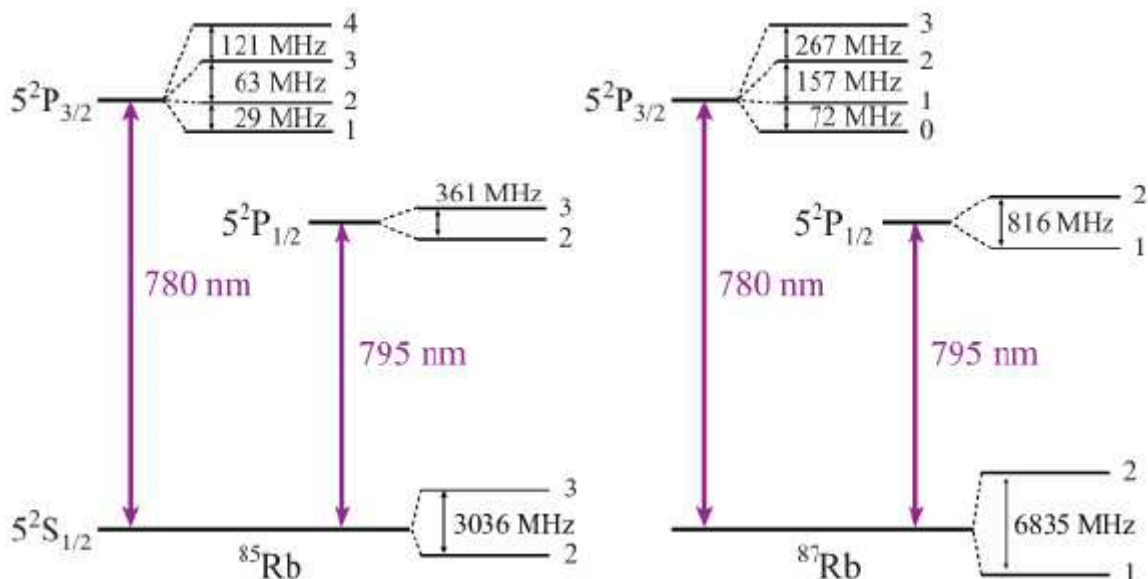


Figure 1. Level scheme of Rubidium.

2.2 Results of Rb sensors

The mixing of rubidium with the background gas is discussed in the following section.

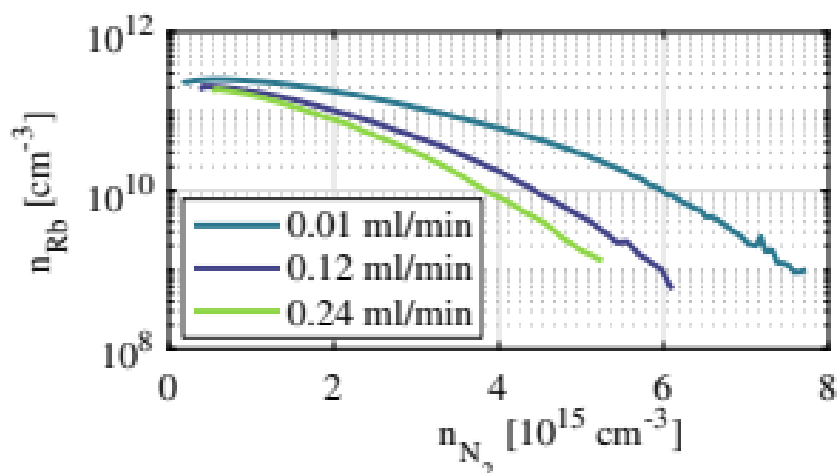


Figure 2: Rb density as function of the N2 density for different filling speeds of the cell with N2.

macQsimal	Title	Deliverable Number D8.2
Project Number 820393	Quantification of bandwidth and sensitivity of Rb sensor for different sample volumes	Version 1

Nitrogen and rubidium are mixed by slowly filling the spectroscopy cell with nitrogen through a mass flow controller. The nitrogen flow is for example 0.12 ml/min. Rubidium is evaporated in a glass reservoir attached to the cell. The reservoir is heated to 90 °C while the spectroscopy cell is heated to 100 °C. The rubidium atoms diffuse into the cell through the background gas. This technique turned out not to be beneficial. For higher buffer gas pressures most of the rubidium condensates on the cell walls instead of flying to the excitation region. It is therefore impossible to set the nitrogen and rubidium partial pressures independently from each other. In addition, the nitrogen flow, i.e., the speed at which the cell is filled is crucial for the final ratio between nitrogen and rubidium. At slow filling rates, the evaporation of rubidium is able to counteract the condensation on the cell walls. However, for larger flows the condensation of rubidium prevails. This is limiting the total speed at which the gas in the cell can be exchanged. A quantitative approximation of the effect is not possible because of the complicated cell geometry.

Another important specification characteristic for the sensor is how fast the charges generated in the cell can be withdrawn from the cell. This will be discussed in the following section.

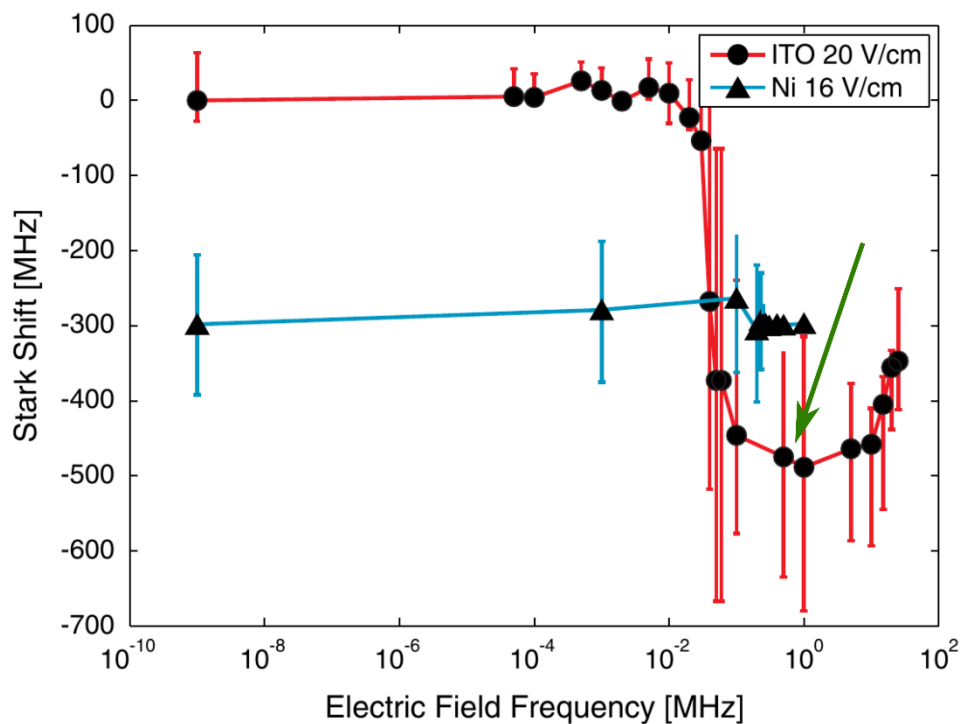


Figure 3: Frequency dependence of the electric field inside small electrically contacted vapor cells. The dots connected with a red line correspond to a cell with ITO coating. The triangles connected via the blue line correspond to a cell coated with nickel. The green arrow indicates the frequency range from which onwards the charges are withdrawn fast enough from the cell to decrease the electric field generated by the charges at the electrodes. From 40 kHz onwards the retrieval of the charges is fast enough to avoid the generation of any additional electric field.

Figure 3 shows that for electric field frequencies smaller than around 1 MHz the charges generated in the cell can be withdrawn fast enough so that the electric field generated by the charges at the electrodes is lowered. For frequencies smaller than 40 kHz the charges are withdrawn so fast that there is no electric field generated by the charges anymore.

The flight time it takes from the excitation until the charges arrive at the electrodes can be estimated for known bias voltages. The counter propagating excitation scheme of the lasers leads mainly to the excitation of atoms and molecules with zero velocity along the propagation path of the lasers. For the estimation of the time of flight only those atoms or molecules are taken into account. In addition, possible collisions between the atoms on the path to the electrodes are neglected. For positively charged ions and

macQsimal	Title	Deliverable Number D8.2
Project Number 820393	Quantification of bandwidth and sensitivity of Rb sensor for different sample volumes	Version 1

electrode distances from 1 mm to 5 cm the time of flight is on the order of microseconds as can be seen on Figure 4. This corresponds to frequencies in the range of several hundred kHz to a MHz seen on Figure 3. Figure 3, which was explained above, shows that our electrodes can remove the charges fast enough. Typical electrode distances for our setups are marked with vertical lines in Figure 4. The red ($d = 0.5$ cm) and black ($d = 1.2$ cm) line correspond to smaller cells with onboard amplifiers. The green and yellow line correspond to larger cells where an external trans-impedance amplifier was used. Hereby the green line ($d = 1$ cm) marks the distance for a simple plate capacitor. The yellow line ($d = 4$ cm) corresponds to a cell with a more complex electrode configuration where a shielding electrode is used to avoid electrons reaching the measurement electrode. For the more complex electrode geometry, the given estimation is no longer valid since the electric field is no longer homogenous. When ionizing the atoms or molecules in the cell, electrons are produced as well. However, we do not consider them in our estimation here, since in the experiment only the ions will be collected for the current detection. Collecting the electrons is less feasible since they are not only generated via the ionization process but also by the photoeffect of the lasers, especially in the case of rubidium, which tends to stick to the cell walls where it is hit by direct and indirect light from the 474 nm laser, whose single photon energy is already larger than the workfunction of bulk rubidium.

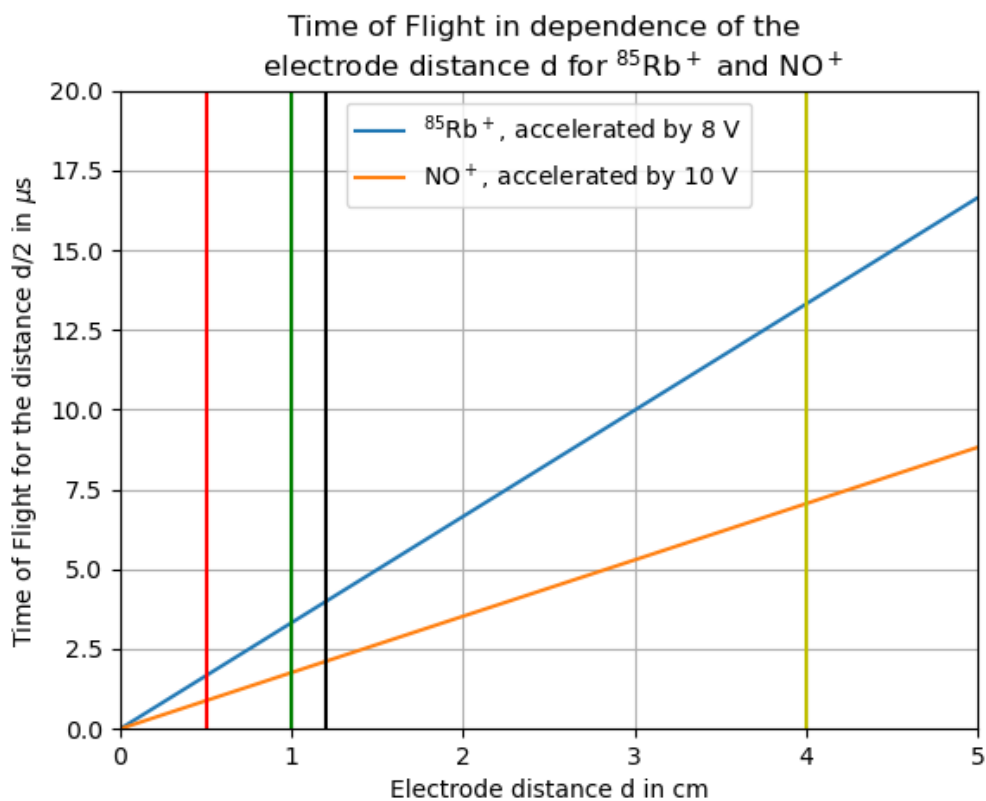


Figure 4: Time of flight for the ions to reach the electrodes in dependence of the electrode distance d . The charges have to travel a distance $d/2$ to the corresponding electrode. The bias voltages are typical for our current measurement setups. The vertical lines mark typical distances between the electrodes. Red line 5 mm, electrically contacted cell, green line 10 mm large cell with plate capacitor inside. Black line 12 mm electrically contacted cell. Yellow line 40 mm, but with shielding electrode.

There are several difficulties which appeared during the investigation of the sensor principle with rubidium which indicate that for further investigation and development nitric oxide is a more suitable candidate. As shown above (cf. Figure 2) the rubidium and nitrogen density are not independent. Since the rubidium density has to be known to characterize the properties of the gas sensor, this is a major

macQsimal	Title	Deliverable Number
Project Number 820393	Quantification of bandwidth and sensitivity of Rb sensor for different sample volumes	D8.2
		Version 1

drawback, especially since for lower rubidium densities an electrical signal can still be measured but the density itself can no longer be determined since the optical signal required to do so is no longer visible. The nitric oxide gas sensor does not suffer from any of those restrictions and is therefore a way better candidate to explore sensing of smaller concentration, i.e., densities.

The rubidium density is also linked to the photocurrent since the coating of the cell walls with bulk rubidium depends also on the rubidium density inside the cell. Measuring the response R of the sensor, which is an important sensor benchmark is not possible in a reliable way under these conditions. In the case of nitric oxide, the photocurrent is no issue since only positive charges are collected via the electrodes in our setup.

2.3 General scheme NO (For details please refer to D8.1)

To mix nitrogen and nitric oxide a gas mixing unit employing four MFCs was build. To ensure a fast exchange of the gas in the spectroscopy setup, the flow through the mixing setup must be viscose. A ballistic flow would result in stronger mixing between the gas mixtures of different concentrations when the MFC settings are changed. This would result in long waiting times since one would have to wait until the system is back in equilibrium, i.e., all pipes are sufficiently rinsed with the newly set gas mixture.

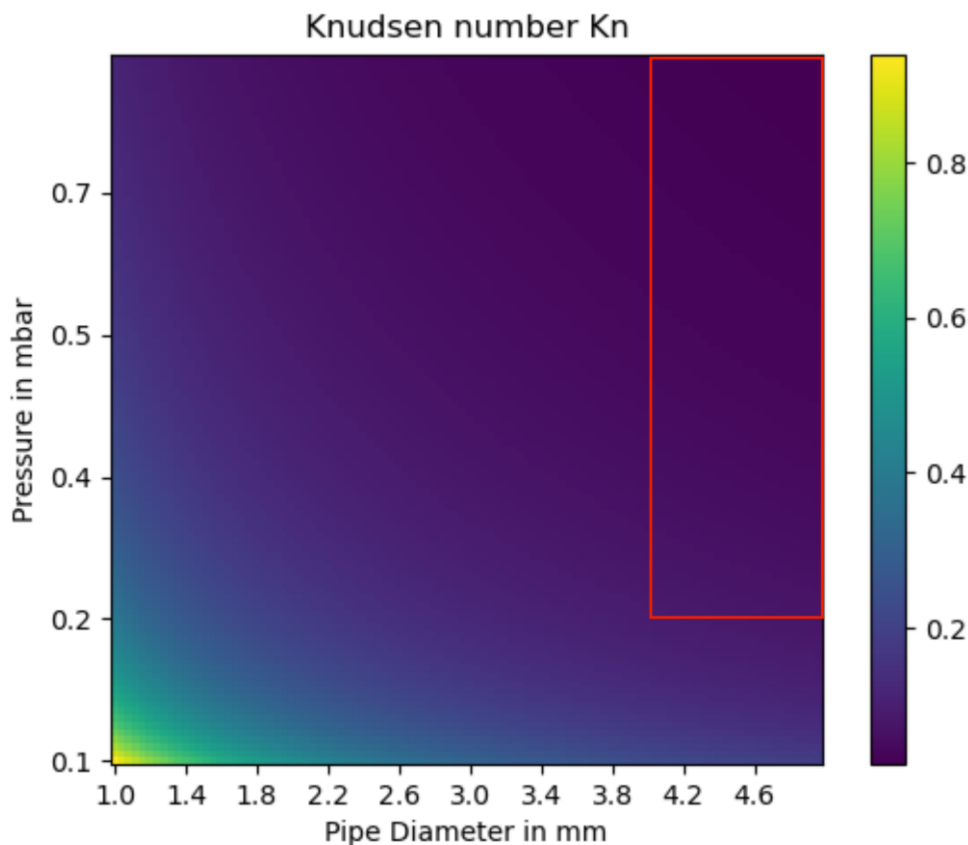


Figure 5: Knudsen number Kn in dependence of the pipe diameter in mm and the pressure in mbar. The pipes of the gas mixing unit are 4 mm in diameter. The red rectangle marks the regime where spectroscopy measurements are typically performed.

Figure 5 shows the Knudsen number for different pipe diameters and pressures. The calculation was performed estimating the mean free path of nitrogen using its collisional cross section. This is a valid approximation since most of the gas flowing through the gas mixing unit will be nitrogen, which is needed to dilute small quantities of nitric oxide. To reach dilution lower than the ppm range we plan to use prediluted nitric oxide (e.g., 100 ppm nitric oxide in nitrogen). This is feasible for safety reasons and

macQsimal	Title	Deliverable Number
Project Number 820393	Quantification of bandwidth and sensitivity of Rb sensor for different sample volumes	D8.2
		Version 1

because it allows us to use the full parameter range of the gas mixing unit. The gas mixing unit is made of pipes with an inner diameter of 4 mm. Typical pressures for the current spectroscopy experiments are between 0.2 mbar and 1 mbar. The typical parameter range is marked with a red rectangle. The Knudsen number is in the range of 0.1 and lower, which corresponds to a mainly viscose flow.

2.4 Vapour cell with current detection

The glass cell is a through-flow cell. The windows are made of quartz glass allowing for a high transmission of all beams. A picture of the currently used cell can be found in Figure 6. Figure 7 shows the electrode configuration used for the detection of free charged particles. The configuration itself has been simulated and optimized within the scope of this project. It maximizes the number of particles detected while keeping the noise due to the photo effect minimal. Since NO is corrosive to several materials special care has been taken in the selection of the former. The cell has been tested thoroughly and meets the performances needed.

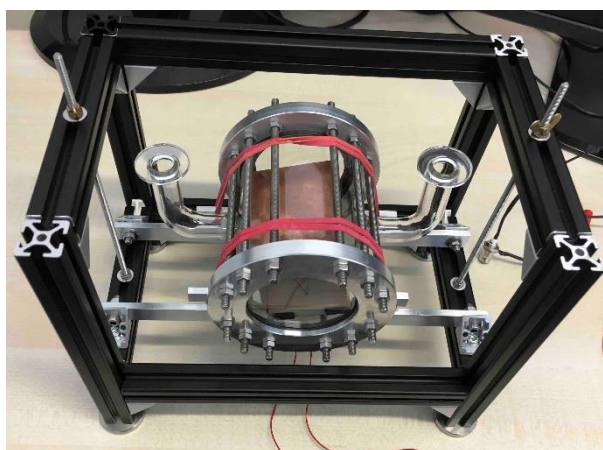


Figure 6: Picture of the through-flow cell removed from the actual laser setup. While the used lasers pass the cell from top to bottom, the gas mixture flows from left to right.



Figure 7: Detailed view at the electrode configuration for current detection. The configuration has been built in such a way that the detection of NO^+ ions is maximized whereas the photo effect is maximally suppressed.

macQsimal	Title	Deliverable Number
Project Number 820393	Quantification of bandwidth and sensitivity of Rb sensor for different sample volumes	D8.2
		Version 1

2.5 Data acquisition

At the current stage, the gas setup consists of two pumps yielding a pressure of 10^{-4} mbar when the system is fully evacuated. Currently all measurements are performed using nitric oxide with a purity of 2.5. The pressure can be adjusted using a needle valve and monitored using a vacuum gauge.

A voltage of about 1 V is applied to the electrodes when measuring. A current preamplifier (Model 1211, DL Instruments) generates the needed amplification before the final signal is monitored on an oscilloscope. Furthermore, a frequency reference (Fabry-Pérot cavity) is set up and monitored for each individual transition.

2.6 Outlook

In D8.3 we will report on the details on the trans-impedance amplifiers and the performance of the NO sensor in different configurations.